

## Oscillating Interatomic Potentials and Growth of Icosahedral Quasicrystals

V. E. Dmitrienko and S. B. Astaf'ev

*A. V. Shubnikov Institute of Crystallography, 59 Leninsky Prospekt, 117333 Moscow, Russia*  
(Received 27 February 1995)

The crucial role of frustration in atomic ordering for quasicrystal formation is demonstrated within a simple pmodel for three-dimensional growth of icosahedral quasicrystals in binary alloys (up to  $2 \times 10^6$  atoms). Two features of the model are important: (1) The ratio of atomic sizes is the one typical for the CsCl structure and (2) the interatomic potential is an oscillating function of interatomic distances (those oscillations cause frustration in atomic ordering). It is shown that different potentials result in different faceting of the grown clusters. Phasonic jumps and the phasonic relaxation in the clusters are discussed.

PACS numbers: 61.44.+p, 05.50.+q, 61.50.Ks

The nature of quasicrystals is still a source of controversy even ten years after their discovery [1]. High-dimensional descriptions have been developed to specify the positions of atoms in quasicrystals [2–4], but the origin of their complicated atomic structures is unclear. It is especially difficult to imagine the growth of quasicrystals because, rigorously speaking, every atomic position has a unique environment and the growth process is nonlocal [5]. However, physical growth algorithms may be practically local at least when artificial units, like the Penrose tiles, are used [6]. More realistic two-dimensional atomic models of quasicrystal growth include atoms of two different sizes [7], but the ratio of those sizes [ $2 \cos(\pi/10) \approx 1.9$ ] is too large for real alloys. Three-dimensional growth models are usually constructed from special atomic clusters (the Ammann rhombohedra, different units with icosahedral symmetry, etc.) which are assembled according to some matching rules. A typical example is the icosahedral glass model which assumes that large icosahedral clusters, found in crystalline approximants, can be linked together in a way which preserves the quasiperiodic translational order (see useful surveys by Stephens and Elser [8,9] and further development by Robertson and Moss [10]).

In this Letter we consider a three-dimensional model of the quasicrystal growth which exploits some general principles of atomic ordering (prompted by the structure of simple crystalline approximants) rather than ready-made clusters. Atoms are supposed to be spherical; only the atomic sizes and interactions are specifically chosen. The model includes two crucial features: (A) a special short-range ordering, *the dodecahedral local ordering* (DLO), probably generated by close packing of atoms with two different sizes; and (B) the oscillatory interatomic potentials which cause frustration between the short-range and medium-range orderings. In the remaining part of this paper, we discuss these two features and then present the properties of the quasicrystalline cluster grown within our model.

The dodecahedral local ordering of atoms is rather unconventional and merits comment (see also [11]). By definition, the DLO is such an ordering when all the closest

neighbors of each atom are positioned at vertices of a regular pentagon dodecahedron. Hence the DLO is similar to the canonical-cell ordering (or *b-c* ordering) of icosahedral clusters developed by Henley [12], but his *b* linkage and *c* linkage are  $\tau^3$  times longer than the two shortest interatomic distances,  $r_2$  and  $r_3$ , of DLO [ $\tau = (1 + \sqrt{5})/2 \approx 1.618$ ]. The center-to-vertex distance of the dodecahedron,  $r_3$ , corresponds to the shortest interatomic bonds directed along threefold axes (in the Al-transition-metal alloys  $r_3 \approx 2.5 \text{ \AA}$  and in the Al-Li-Cu alloys  $r_3 \approx 2.7 \text{ \AA}$ ). The length of the bonds directed along twofold axes  $r_2$  is only 15% more,  $r_2 = 2r_3/\sqrt{3}$ ;  $r_2$  is the distance between *next-neighboring* vertices of the dodecahedron. These two typical distances are simply related with the quasilattice constant  $a_R$ ,  $a_R = r_2\sqrt{\tau + 3/4}$ . The distance between *neighboring* vertices of the dodecahedron is  $r_2/\tau$ ; it is significantly shorter than normal interatomic distances and only a couple of the twenty vertices are simultaneously occupied ( $\leq 8$ ). The bcc and CsCl crystals are trivial examples of the DLO (Fig. 1); in other crystals (FeSi, Hg,  $\alpha$ -Al-Mn-Si,  $R$ -Al<sub>5</sub>Li<sub>3</sub>Cu, etc.), which are the approximants of icosahedral quasicrystals, the DLO is a result of special atomic positions and/or special unit-cell parameters. Within the six-dimensional projection scheme, a high-density DLO quasicrystal arises if its acceptance domain has the form of the ruffled truncated triacontahedron [13–15], and the DLO motives were really found in the icosahedral quasicrystals of different composition (Al-Mn-Si [2], Al-Fe-Cu [3], Al-Pd-Mn [4]).

This unusual ordering may be caused by the close packing of atoms with two different sizes, large (*L*) and small (*S*), so that the interatomic distances correspond just to the DLO:

$$r_{LL} = r_2, \quad r_{LS} = r_3. \quad (1)$$

Notice that the difference in atomic sizes increases the atomic packing fraction in comparison with one-component DLO structures: For the case given by Eq. (1), this increase reaches its maximum (about 17%). The equilibrium  $r_{SS}$  distance seems to be of minor

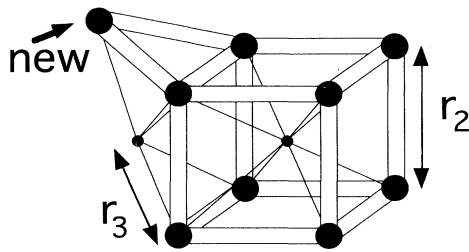


FIG. 1. A simple example of DLO growth: new large atom, added to the initial CsCl cluster, violates the crystalline ordering. This way the outer shell of the Mackay icosahedron may be constructed around the initial cluster [11]. Single (double) lines correspond to threefold (twofold) icosahedral axes.

importance because the positions of small atoms are really fixed by three or more *LS* bonds. During the growth, *L* and *S* atoms may be stuck one by one so that (a) every new atom would be in contact with at least three old atoms (Fig. 1), and (b) the interatomic distances would be in accordance with Eq. (1) (a distorted tetrahedral packing). This way the DLO structures can be obtained but, unfortunately, wrong positions can also arise in the packing: For instance, a regular tetrahedron of four *L* atoms produces non-DLO positions.

Perhaps there should be some additional mechanism which suppresses non-DLO atomic configurations, but it is not the aim of the present consideration. Here we simply *postulate* the DLO in growing clusters and address another part of the problem: What is the mechanism which selects between quasicrystalline and crystalline DLO structures? It will be shown that the oscillating interatomic potentials, typical for metals, may be responsible for the selection. Their importance for the stability of quasicrystals was demonstrated earlier [15–17] (for more wide applications, see [18,19]). Those oscillations are a result of electronic contribution to the interatomic forces, and the Friedel wavelength of the oscillations,  $\lambda_{FO}$ , is determined by the Fermi momentum  $k_F$  ( $\lambda_{FO} = \pi/k_F$ ). The electronic effects are frequently dominant in quasicrystals [20]; however, to our knowledge, they have never been used in the growth models.

Our computer simulations are based on the Eden model of alloy quenching previously used for decagonal quasicrystals [7,21]; it means that any atom, being once attached to the “best” position, has no further move (perhaps a more realistic approach may be obtained within molecular dynamics simulations [22]). The growth process begins with a seed DLO cluster (3–50 atoms). Then, according to the postulated DLO, trial positions are generated at all vertices of the coordination dodecahedron around each atom. Every next atom is stuck to the trial position of the lowest energy; this rule is not local, but it means physically that the position with the lowest energy has a much larger sticking coefficient [6]. If there are several positions with the lowest energy, then

we add the atom to the first found one. In the present simulations we ignore those positions, which correspond to six-dimensional body centers [2–4], because they give only about (3–5)% of all atoms. Geometrically our model is similar (with the factor  $\tau^{-3}$ ) to the icosahedral glass models [8–10], but it has another physical content.

The most decisive step is the selection of the trial positions by energy. Here it is supposed that the energy  $E$  of a trial position is proportional (a) to the number of atomic bonds,  $N_{\text{bond}}$ , relating this position with the atoms of the cluster, and (b) to the energy of each bond,  $E_{\text{bond}}(r_{\text{bond}})$ , which depends only on the bond length  $r_{\text{bond}}$  but not on the bond direction:

$$E = \sum_{\text{bond}} N_{\text{bond}} E_{\text{bond}}(r_{\text{bond}}). \quad (2)$$

A detailed analysis of “realistic” potentials  $E_{\text{bond}}(r)$  is beyond our computer facilities; therefore, the simulations are performed for several model potentials to understand which parameters are most important. The potentials are assumed to be local:  $E_{\text{bond}}(r) = 0$  if  $r > 2r_3 \approx 5 \text{ \AA}$  and  $E_{\text{bond}}(r) = +\infty$  if  $r < r_3$  (the hard core). In this range, DLO generates only a few different  $r_{\text{bond}}$ : (i)  $r_3$  and  $r_2$  (the first shell), (ii)  $\sqrt{7/4} r_2$  and  $\sqrt{2} r_2$  (the first gap shell), (iii)  $\sqrt{\tau + 3/4} r_2 = a_R$  and  $\tau r_2$  (the outer shell of the Mackay icosahedron), and (iv)  $\sqrt{11/4} r_2$  and  $\sqrt{3} r_2$  (the second gap shell).

We assign the following energies to the bonds:  $E_3 = E_{\text{bond}}(r_3)$ ,  $E_2 = E_{\text{bond}}(r_2)$ ,  $E_{1g} = E_{\text{bond}}(\sqrt{7/4} r_2) = E_{\text{bond}}(\sqrt{2} r_2)$ ,  $E_M = E_{\text{bond}}(\sqrt{\tau + 3/4} r_2) = E_{\text{bond}}(\tau r_2)$ , and  $E_{2g} = E_{\text{bond}}(\sqrt{11/4} r_2) = E_{\text{bond}}(\sqrt{3} r_2)$ ; it seems natural to assign the same energy to the bonds with almost the same  $r_{\text{bond}}$ . Therefore each model potential is characterized by a string of five energies:  $E_{\text{bond}}(r) = (E_3, E_2, E_{1g}, E_M, E_{2g})$ ; really, we have four independent parameters, because the common factor is not important. To speed up the calculations, all the energies are assumed to be dimensionless integers.

The analysis of the ideal quasicrystalline structures and experimental data [2–4,16] shows that the distances (ii) and (iv) correspond to the gaps in the radial atomic distributions; hence the name “the gap shells.” On the other hand, those distances are rather common for the CsCl structure. To suppress the growth of crystalline structures and to obtain those gaps in the growing clusters, we assume that  $E_{1g}$  and  $E_{2g}$  are positive; whereas  $E_3$ ,  $E_2$ , and  $E_M$ , which correspond to dense-populated shells, are negative. For such potentials, we have typical structural frustration; the most dense local order (CsCl) is not favorable at medium-range distances. This can result in more complicated DLO structures, where the frustration is partly relieved because those unfavorable distances are minor or even absent.

The first potential (case I) is  $E_{\text{bond}}(r) = (-1, -1, 0, 0, +\infty)$ ; it means that the distances corresponding to the second gap shell are forbidden because they cost infinite energy. The total energy of allowed

positions is proportional to the sum of  $r_3$  and  $r_2$  bonds (for case I, the preliminary results have been published elsewhere [23]). Notice that larger forbidden distances (about 13 and 18 Å) have been used in the icosahedral glass models [10]. The clusters (up to  $2 \times 10^6$  atoms) grown with this potential have well-defined fivefold facets with growth steps (Fig. 2). The steps correspond to dense-populated puckered atomic planes normal to fivefold axes. Such a pentagon dodecahedron shape is rather common for our model within a wide range of parameters.

If  $E_{\text{bond}}(r) = (-1, -1, 0, 0, E_{2g})$  and  $E_{2g} \leq 0$ , then the growth process gives CsCl-type clusters. However, even a small positive value of  $E_{2g} \approx 0.2|E_2|$  destroys the growth of the CsCl structures in favor of aperiodic structures; hence the growth is very sensitive to the value of  $E_{2g}$ . In

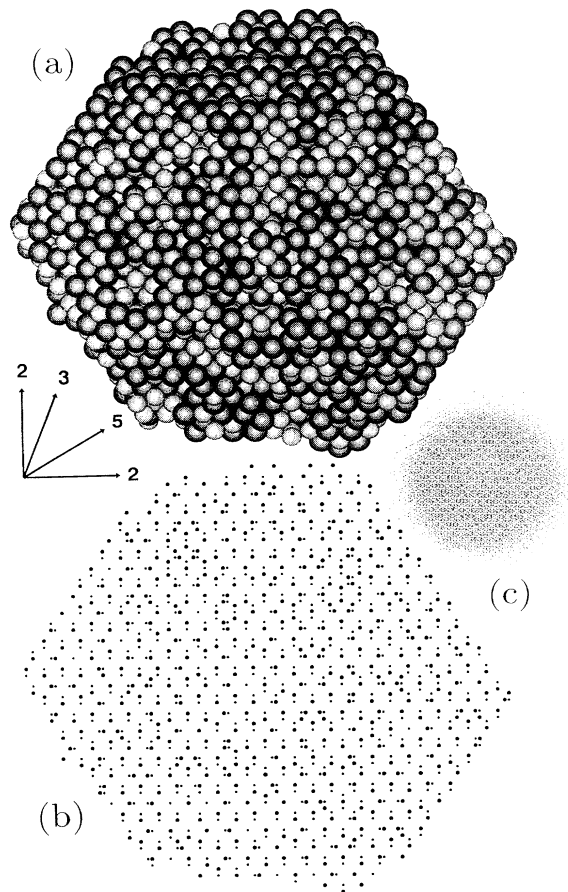


FIG. 2. The view along a twofold axis on the quasicrystalline cluster (case I, 6000 atoms). (a) The  $L$  and  $S$  atoms are drawn in proper scale; the  $L$  atoms are darker; numerous five-atom rings can be found on the fivefold facets. (b) Atoms are drawn as points to show the atomic planes normal to fivefold, twofold, and threefold directions; the directions correspond to numbered arrows. (c) The twofold view in the perpendicular space ( $1.5 \times 10^5$  atoms); it is practically the same for the  $L$  and for the  $S$  atoms.

contrast,  $E_{1g}$  is not so important. Small changes of  $E_{1g}$  produce a minor effect if other  $E_i$  are fixed.

Some of the oscillating potentials [for instance,  $E_{\text{bond}}(r) = (-9, 0, 1, -4, 1)$ , case II] result in clusters with rounded threefold facets (an icosahedron shape). The analysis of possible faceting shapes, similar in a way to cluster model [24], will be given elsewhere.

Several tests have been applied to investigate the quality and average icosahedral symmetry of the grown clusters. First, we have found practically no differences in the relative frequencies of the twenty shortest bonds  $r_3$  (both for whole clusters and for different growth directions). Second, the average coordination numbers for different interatomic distances,  $N(r)$ , are approximately the same for cases I and II and similar to those found for the Al-Cu-Fe quasicrystals [3]:  $N(r_3) \approx N(r_2) \approx 6$ ,  $N(r_{1g}) \approx 4$ ,  $N(a_R) \approx 8$ ,  $N(\tau r_2) \approx 14$ , and  $N(r_{2g}) \ll 1$ . In comparison with the ideal Mackay icosahedron, where  $N(a_R) = 12$  and  $N(\tau r_2) = 30$ , this shell is more than half populated and many large fragments of the outer shells of the Mackay icosahedra may be found.

For more sophisticated tests, we have used the diffraction patterns (Fig. 3) and the six-dimensional embedding of grown clusters [Figs. 2(c) and 4]. The normalized intensities of reflections,  $I(\mathbf{q})$ , are calculated as  $I(\mathbf{q}) = |\sum f_k \exp(i\mathbf{q} \cdot \mathbf{r}_k)| / N^2$ , where  $f_k$  and  $\mathbf{r}_k$  are the atomic scattering factor and the position of the  $k$ th atom,  $f_k = f_L$  or  $f_S$ ,  $f_S + f_L = 1$ ,  $\mathbf{q}$  is a wave vector, and  $N$  is the total number of atoms. The concentrations of  $L$  and  $S$  atoms are not predetermined, but in the grown clusters they are almost equivalent; and therefore the quasilattice is automatically face centered ( $L$  and  $S$  atoms correspond to two sublattices); this leads to  $\tau$  inflation for the fivefold and threefold reflections. The widths of peaks are determined mainly by finite sizes of the clusters; hence our growth process preserves a nonperiodic *translational* order. Nevertheless, slightly different positions, widths, and heights of the peaks provide evidence for phasonic disorder.

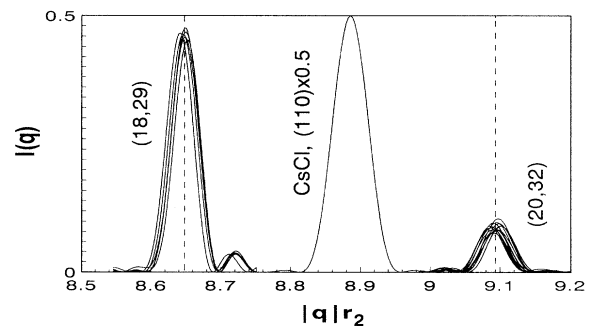


FIG. 3. Simulated diffraction patterns for a cluster of about  $2 \times 10^6$  atoms (case I, atomic scattering factors:  $f_L = 1.3$ ,  $f_S = 0.7$ ). Longitudinal scans are plotted for all icosahedrally equivalent peaks [six fivefold (18,29) and fifteen twofold (20,32) reflections]. Dashed lines mark the exact icosahedral peak positions. For reference, the (110) reflection from the CsCl crystal ( $2 \times 10^6$  atoms) is also shown.

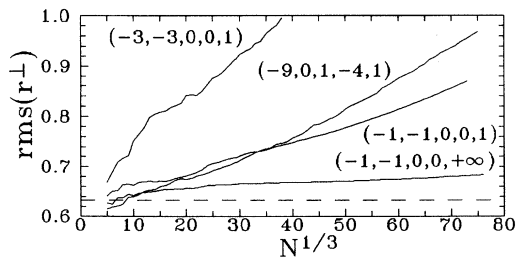


FIG. 4. The root-mean-square perpendicular radius  $\text{rms}(r^\perp)$  as a function of the cluster size in the physical space  $N^{1/3}$  for different interatomic potentials (without relaxation). The dashed line corresponds to an ideal quasicrystal.

This phasonic disorder becomes especially evident if the grown cluster is embedded into a six-dimensional cubic lattice so that the position of any atom in the perpendicular space,  $\mathbf{r}^\perp$ , is determined by its position in the physical space,  $\mathbf{r}$ . In the ideal quasicrystals,  $\mathbf{r}^\perp$  is restricted by an acceptance domain. In the grown clusters, the distribution of  $\mathbf{r}^\perp$  is almost spherical and well localized [see Fig. 2(c)]; a rather rare halo surrounds a dense central part. Hence our real-space growth process results in something like a fuzzy acceptance domain in the perpendicular space; the domain size may be characterized by the root-mean-square radius which increases with increasing  $\mathbf{r}$  (see Fig. 4). Such nonsharp boundaries can be responsible for decreasing the peak intensities and for the diffuse scattering observed in quasicrystals [25].

In the grown clusters, as in ideal quasicrystals, a specific atomic movement, connected with phasonic jumps, is possible: many atoms can jump to other positions, either along twofold directions or along fivefold directions (the corresponding jump lengths,  $r_2\tau^{-1}$  and  $a_R\tau^{-3}$ , are shorter than interatomic distances). Owing to the jumps, the phasonic “relaxation” can be simulated; namely, it is supposed that a phasonic jump is allowed only if its final position has lower energy than the initial one (the interatomic potential is the same as at the growth stage). Being completely three dimensional, the relaxation process nevertheless improves the six-dimensional image of the cluster. More frequently, atoms jump to positions with smaller  $r^\perp$ . However, the overall improvement is not significant; perhaps another potential and/or a thermalization process should be used at the relaxation stage.

In summary, we have shown that imperfect quasicrystalline structures can grow as a result of frustration between short-range and medium-range interatomic forces. The grown clusters are faceted at the macroscopic scales; they correspond to a face-centered icosahedral lattice, and they can relax via phasonic jumps.

We are indebted to L. Pauling, who attracted our attention to the importance of interatomic potentials. We thank A. A. Chernov, M. A. Fradkin, V. L. Indenbom, and M. Kléman for discussions, and O. Laventovich and

R. Lifshitz for their help in manuscript preparation. This work was supported by The International Science Foundation (the travel grant and long-term grant M5B000) and by Université Pierre et Marie Curie (Paris VI). The 486DX2/66 computer, donated by the Alexander von Humboldt Foundation, was used in the simulations.

- [1] D. Shechtman *et al.*, Phys. Rev. Lett. **53**, 1951 (1984).
- [2] C. Janot *et al.*, in *Quasicrystalline Materials*, edited by Ch. Janot and J. M. Dubois (World Scientific, Singapore, 1988), p. 107.
- [3] M. Cornier-Quiquandon *et al.*, Phys. Rev. B **44**, 2071 (1991).
- [4] M. Boudard *et al.*, J. Phys. Condens. Matter **4**, 10149 (1992).
- [5] R. Penrose, in *Aperiodicity and Order: Introduction to the Mathematics of Quasicrystals*, edited by M. Jaric and D. Gratias (Academic Press, San Diego, 1989), Vol. 2, p. 53.
- [6] G. Y. Onoda *et al.*, Phys. Rev. Lett. **60**, 2653 (1988); P. J. Steinhardt, in *Springer Series in Solid-State Sciences: Quasicrystals*, edited by T. Fujiwara and T. Ogawa (Springer-Verlag, Berlin, 1990), Vol. 93, p. 91.
- [7] B. Minchau, K. Y. Szeto, and J. Villain, Phys. Rev. Lett. **58**, 1960 (1987); K. Y. Szeto and Z. M. Wang, Phys. Rev. B **41**, 1347 (1990).
- [8] P. W. Stephens, in *Aperiodicity and Order: Extended Icosahedral Structures*, edited by M. Jaric and D. Gratias (Academic Press, San Diego, 1989), Vol. 3, p. 37.
- [9] V. Elser, in *Aperiodicity and Order: Extended Icosahedral Structures*, edited by M. Jaric and D. Gratias (Academic Press, San Diego, 1989), Vol. 3, p. 105.
- [10] J. L. Robertson and S. C. Moss, Phys. Rev. Lett. **66**, 353 (1991); Z. Phys. B **83**, 391 (1991).
- [11] V. E. Dmitrienko, J. Phys. (Paris) **51**, 2717 (1990); JETP Lett. **55**, 391 (1992); J. Non-Cryst. Solids **153&154**, 150 (1993); Acta Crystallogr. Sect. A **50**, 515 (1994).
- [12] C. L. Henley, Phys. Rev. B **43**, 993 (1991).
- [13] C. L. Henley, Phys. Rev. B **34**, 797 (1986).
- [14] M. Duneau and C. Oguey, J. Phys. (Paris) **50**, 135 (1989).
- [15] A. P. Smith, Phys. Rev. B **42**, 1189 (1990); **43**, 11635 (1991).
- [16] J. Hafner and M. Krajčí, Europhys. Lett. **13**, 335 (1990); J. Non-Cryst. Solids **150**, 337 (1992); M. Krajčí and J. Hafner, Phys. Rev. B **46**, 10669 (1992).
- [17] Z. Olami, Phys. Rev. Lett. **65**, 2559 (1990).
- [18] J. Hafner, *From Hamiltonians to Phase Diagrams* (Springer-Verlag, Berlin, Heidelberg, 1987), p. 34.
- [19] R. Phillips *et al.*, Phys. Rev. B **49**, 9322 (1994).
- [20] S. J. Poon, Adv. Phys. **41**, 303 (1992).
- [21] Z. Olami, Europhys. Lett. **16**, 361 (1991).
- [22] M. Dzugutov, Phys. Rev. Lett. **70**, 2924 (1993).
- [23] V. E. Dmitrienko and S. B. Astaf'ev, JETP Lett. (to be published).
- [24] T. Lei and C. L. Henley, Philos. Mag. **B63**, 677 (1991).
- [25] M. de Boissieu *et al.*, Phys. Rev. Lett. **72**, 3538 (1994).

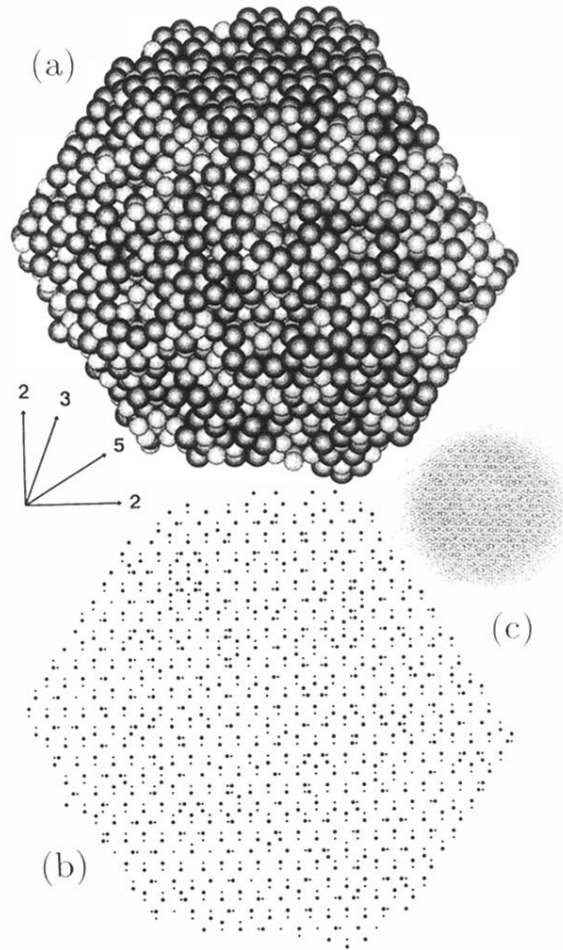


FIG. 2. The view along a twofold axis on the quasicrystalline cluster (case I, 6000 atoms). (a) The  $L$  and  $S$  atoms are drawn in proper scale; the  $L$  atoms are darker; numerous five-atom rings can be found on the fivefold facets. (b) Atoms are drawn as points to show the atomic planes normal to fivefold, twofold, and threefold directions; the directions correspond to numbered arrows. (c) The twofold view in the perpendicular space ( $1.5 \times 10^5$  atoms); it is practically the same for the  $L$  and for the  $S$  atoms.